CONF-8303199--1

DE85 012622

# "MEDICAL APPLICATIONS OF NMR IMAGING AND NMR SPECTROSCOPY WITH STABLE ISOTOPES"

SUMMARY OF SYMPOSIUM
COSPONSORED BY
THE AMERICAN COLLEGE OF NUCLEAR PHYSICIANS
AND
THE U. S. DEPARTMENT OF ENERGY
HELD ON
12 MARCH 1983 AT DORADO, PUERTO RICO

By N. A. Matwiyoff, Los Alamos National Laboratory

## I. INTRODUCTION

Nuclear magnetic resonance, NMR for short, is being used in medicine and biomedical research in two different ways:

(1) Proton NMR imaging is providing anatomical details at a high degree of resolution (<1 mm), soft tissue contrast being a hallmark of the method; and

(2) NMR spectroscopy, especially of the phosphorus-31 and carbon-13 isotopes, is providing quantitative information about biochemical reactions as they occur in defined volumes deep within the tissues of live animals or perfused organs.

A very important feature about NMR as a diagnostic and research tool is that the measurements are essentially non-invasive -- the subject is placed in a low energy magnetic field and the data for images or spectra are received by remote coils.

NMR has been used as a non-destructive analytical technique in physics and chemistry for almost four decades. Its application to

## DISCLAIMER

living systems has occurred within the last decade, and its use in medicine only within the last two to three years. NMR relies on the magnetic properties of the nuclei of certain isotopes that possess a nuclear magnetic moment. In the presence of a static magnetic field, the nuclear moment, like a microscopic bar magnet, can assume only fixed orientations. Several of the most commonly used nuclei in NMR - $^{1}H$, $^{13}C$, $^{31}P$ - have nuclear spin 1/2 and their magentic moments can adopt only two orientations, a low energy one aligned with and a high energy one opposed to, the applied static magnetic field.

When a collection of these nuclei is placed in a magnetic field ($H_0$), there is a slight excess of nuclear moments ($M_0$) which are oriented along the $H_0$ direction and precess around it at a characteristic frequency, called the Larmor frequency (Fig. 1). The Larmor frequency is proportional to the product of the strength of the nuclear magnetic moment and the strength of the applied static field. In the NMR experiment, the magnetization $M_0$ is detected by applying a second magnetic field in the form of a radiofrequency pulse ($H_1$, Fig. 1) at the Larmor frequency which causes $M_0$ to rotate away from the Z axis. As a result, a fluctuating magnetization is induced in the x, y plane and this resonance is detected as a voltage by a very sensitive radiofrequency pick-up coil. In practice, to improve the signal to noise ratio, many pulses are applied with a suitable time interval between them, and the signals are averaged in a computer.

In an external field of 1 Tesla, protons ($^{1}H$) resonate in a narrow band of frequencies near 42.6 MHZ, $^{13}C$ at 10.7 MHZ, and $^{31}P$ in a narrow band near 17.2 MHZ. Resonance occurs in a narrow band of frequencies rather than at a single frequency because the static applied magnetic field is partially shielded from the nucleus by the electrons surrounding the nucleus. This phenomenon, called the chemical shift, is the basis for NMR spectroscopy.

Nuclei in electron rich areas of molecules resonate at slightly lower frequencies than nuclei in electron poor regions. The range of frequency shifts for most nuclei is on the order of parts per million

(PPM) of the Larmor frequency and chemical shifts are usually reported in PPM with respect to a reference. The chemical shifts for the $^{13}C$ NMR spectra reproduced in Fig. 2 were measured with respect to the $^{13}C$ resonance of the standard reference compound, tetramethylsilane [$(CH_3)_4Si$, TMS]. The natural abundance of $^{13}C$ is 1.1 atom % but more than 20 Kg/yr are enriched to the 99 atom % level in the DOE supported isotope separation facilities at Los Alamos where isotopically enriched compounds are also prepared for metabolism studies.

The $^{13}C$ spectra in Fig. 2 show that the perfused liver is actively transforming labeled alanine into glutamate and glucose. Of course, these are well known reaction pathways for liver which transforms alanine into pyruvate, the substrate for gluconeogenesis (the synthesis of new glucose) or for entry into the Krebs cycle which produces the cells' energy and makes glutamate as an important regulatory by-product. What is new, is that NMR spectroscopy tracks these processes non-destructively in living cells while they are actually occurring. NMR spectroscopy can be applied to systems of varying complexity, allowing the study of isolated enzyme systems, perfused organs, and intact animals.

Proton density imaging, at the present stage of development, depends on the high concentration of water protons, and protons attached to carbon ($CH_2$) in carboxylic acids of mobile lipids in the body. Further these $H_2O$ and $CH_2$ protons have very small chemical shifts and resonate at nearly the same frequencies at a given point in the body under the conditions of the imaging experiment. A spread of resonance frequencies for these protons is then induced by imposing a gradient on the static magnetic field such that the $^1H$ resonance from different regions of the object appear at slightly different frequencies, varying by perhaps one part in a thousand. This frequency variation, as illustrated in Fig. 3, can be translated into spatial variations and converted into an image. To generate a planar or two dimensional image (a thin slice through the body), one method employed is to rotate magnetic field gradients within the plane, generating signals which may be regarded as one dimensional projections of the

profile of proton density. Back projection of these profiles then allow reconstruction of the image with algorithms and filter functions similar to those employed in x-ray CT imaging, the intensity distribution of NMR frequencies taking the place of x-ray attenuation profiles. Unlike x-ray CT units, NMR imagers need no moving parts because a magnetic field gradient can be generated in any direction by a computer controlled change in the current of gradient coils oriented in the x, y, and z directions. Also in contrast to x-ray CT images, the resolution and contrast of a proton image is strongly influenced by the timing and type of the NMR excitation pulses and the time delay between the pulse and data collection.

These time dependent contrast effects occur because the sample magnetizations $M_0$ and $M_{xy}$ change with time on a scale that can be made comparable with data collection times and the time required to prepare the magnetization of the sample with the appropriate pulse(s). The change of the sample magnetization with time is called relaxation and is illustrated in Fig. 4. The processes, characterized by the $T_1$ and $T_2$ relaxation times depicted in Fig. 4, are brought about by intrinsic magnetic fields in the sample which vary with time because of molecular motions whose frequency is near the Larmor frequency. The intrinsic fields are usually caused by adjacent magnetic dipoles. $T_1$ and $T_2$ in liquids and soft tissue depend on the size of the molecules containing the nuclear spin, and the rate at which they are rotating or tumbling. For example, relaxation times are shorter in white matter than in grey matter because white matter contains a larger percentage of faster relaxing lipid protons. Similarly, tissues whose mobile detectable protons are mainly those of water, can also show large differences in $T_1$ and $T_2$ depending on how tightly water is bound to large protein molecules and how much of it is bound. Typical $T_1$ and $T_2$ values are on the order of 2 seconds for pure water and hundreds of milliseconds for water in biological tissues.

A simple illustration of image enhancement by selecting $H_1$ pulses that weight the $T_1$ differences of samples is illustrated in Fig. 5. This type of image enhancement or contrast is called <u>partial saturation</u>

recovery. Other weighting schemes whose full description is beyond the scope of this summary include:

(1) Inversion recovery contrast. This also is a $T_1$ weighted technique which uses a two pulse sequence; and

(2) Spin echo contrast. This is a pulse and detection sequence which weights $T_2$.

Unlike the $T_1$ weighted images where short $T_1$ values enhance contrast, mobile proton in tissues with long $T_2$ values are enhanced (appear as brighter areas) in spin echo methods. Because the image contrast is a sensitive function of $T_1$, $T_2$, the proton density, and the pulse interval selected, it is important to have quantitative data on the $T_1$ and $T_2$ of diseased and normal tissue. These $T_1$ and $T_2$ studies are still in their very early stages.

Finally, although a full description is also outside the scope of this summary, it should be noted that rapid progress is being made in developing two and three dimensional Fourier transform imaging. In contrast to the projection reconstruction techniques outlined here, these methods offer the advantage that image quality is less affected by magnetic field inhomogeneities and motion.

In the following, the current status of NMR imaging and NMR spectroscopy are summarized using, for the most part, examples from the March 1983 Puerto Rico symposium.

## II. NMR IMAGING

Even at this very early stage of its development, proton NMR imaging is capable of providing anatomical details that are at least as useful in medical diagnosis as those obtained from x-ray CT images. A detailed analysis of the comparative predictive utility of proton NMR, x-ray CT, and other imaging modalities using data from patients with clinically well defined diseases is not yet published. However,

preliminary reviews of images obtained on a limited number of patients at the Massachusetts General Hospital and the University Hospital, Cleveland, are very encouraging. For example, for twenty-five stroke patients studied at Massachusetts General, CT and NMR images unequivocally revealed the abnormalities in 20 of the patients, three of them were judged normal on the basis of CT and NMR images, and in two, the abnormalities were revealed by the NMR images but not the CT scans. At University Hospital, for 16 patients studied, NMR and CT images revealed lesions in the chest cavity equally well in 11 patients, NMR images proved superior to CT in four of the patients, and in one of the patients the CT image proved superior to the NMR image. Similar results have been obtained in studies of brain tumors and neoplasms of liver in small patient populations.

For one disease at least, multiple sclerosis (MS), NMR imaging presents a distinct advantage. It reveals demyelination, loss of white matter, much more clearly than CT images do. Recent studies of a patient having an MS attack and having had a history of two older attacks, provided NMR images of the brain in which the MS plaques could be dated! This opens the possibility of using NMR imaging to monitor the course of MS therapy, this being of particular importance because the disease has an undetermined etiology and there is no effective therapy for it now. These data suggest the potential utility of NMR for monitoring therapy in a variety of disease processes.

Contrary to early reports, the normal pancreas can be imaged by proton NMR but, somewhat surprisingly, it is very difficult at this stage of development of the technique to distinguish in proton NMR images the soft tissue calcification that occurs in some inflammatory diseases of the pancreas. Proton NMR imaging also failed to reveal the lesion in one well defined case of a calcification of a lymph node. These observations, and the fact that inversion recovery NMR methods provide better contrast than saturation recovery with the pulse intervals commonly used, highlights the importance of obtaining quantitative $T_1$ and $T_2$ values of diseased and normal tissues so that the optimum pulse sequence and pulse intervals to be used for NMR imaging of

specific suspected pathologies can be specified. At stake is the fact that the inversion recovery method provides contrast superior to saturation recovery, but takes considerably more time.

For the longer term, paramagnetic compounds targeted to bind to specific tissues offer promise as agents to enhance contrast in proton NMR imaging and to assess some physiological function of organs. Paramagnetic compounds contain unpaired electrons which generate intense fluctuating magnetic fields in their immediate vicinity (within 10 Å of the paramagnet), fields which strongly influence $T_1$ and $T_2$. Paramagnetic contrast agents under initial study with animal models include iron and manganese chelate compounds and organic compounds containing the nitroxide (N-O) moiety which has an unpaired electron. Animal model and a few human studies have shown that iron chelates and nitroxide compounds can markedly enhance contrast in NMR images of organs at doses which are biologically acceptable. The development of magnetic bullets is a realistic possibility in the long term, the paramagnetic agents being attached chemically to antibodies for specific tissues or to other chemically synthesized carriers which discriminate between normal and diseased tissue. In this area, there is a need for DOE, NIH, and other interested agencies to identify, support, and coordinate the chemical and biochemical synthesis efforts which will supply the future NMR contrast agents and the diagnostic and therapeutic radiopharmaceuticals. The chemical and biochemical synthesis methodologies in these two areas of nuclear medicine are similar; and efforts to coordinate and synergize them will reap disproportionate rewards.

One promising area for development in NMR imaging using $T_1$, $T_2$, and chemical agents for contrast is the investigation of blood flow effects. Although flow imaging is still in its infancy, the early results on animal models and select human subjects suggest that the method will be refined rapidly to permit the clinician to quantitate the vessel flow distributions within the human body which will facilitate the diagnosis of vascular disease. Although NMR imaging can provide information about blood flow to tissue, it cannot directly

assess whether tissues having an adequate blood supply are functioning normally - that is take up oxygen and consume it in metabolic reactions at normal rates. This assessment can be made using NMR spectroscopic techniques for metabolic profiling outlined in the next section of this report.

The optimum strength of the static magnetic field, $H_0$, for NMR imaging is currently the subject of considerable controversy. Most human, whole body NMR images have been obtained at static field strengths of 0.1-0.15 Tesla. However, recent studies by researchers at the University of California, San Francisco and University Hospital, Cleveland, show that NMR images obtained at 0.35 Tesla have better spatial resolution and can be obtained in shorter "scan" times, both results being expected on theoretical grounds. On these same theoretical grounds, one would opt for NMR imaging systems at the highest possible static magnetic field strengths. However, practical considerations intrude. One of these is associated with the fact that the radiofrequency field, $H_1$, necessary to record proton images begins to be severely attenuated (absorbed) by large dielectrics such as the human torso, at static fields approaching 2 Tesla. These attenuation effects, unless compensated for, can distort the image. Another practical consideration that serves to limit the strength of the magnetic field used in NMR imaging studies, is the fact that the site requirements and their costs increase with the magnetic field strength used. At high magnetic fields, ferromagnetic materials in the environment can degrade the quality of the NMR image by changing the shape of the $H_0$ field. These ferromagnetic materials include steel in reinforced concrete floors, elevators, and passing automobiles. Currently two types of magnets are being used in NMR imaging. An air core resistive electromagnet is appropriate for proton imaging at field strengths of 0.2 Tesla or less since power consumption (~50 kW) and cooling requirements are not prohibitive. Field strengths above 0.2 Tesla are best generated by superconducting magnets which consume little electrical power but require the expensive cryogenic fluids, liquid nitrogen and liquid helium. The combination of these considerations demands a careful consideration of the balance of

equipment, building, and operational costs in the selection of an NMR imager. Of course, if one wants to combine imaging with NMR spectroscopy, then a high field (1.5 Tesla or above) system is required. One practical long range planning approach is to acquire a super conducting system which will allow fields of 1.5 T but can be operated at 0.5 T for routine proton imaging.

## III. NMR SPECTROSCOPY

Phosphorus-31 NMR spectroscopy has been used extensively in humans, animal models, and perfused organs to study energy metabolism, especially in muscle. In muscle which functions normally, the chemical sources of energy are:

$$ATP \longrightarrow ADP + P_i + ENERGY$$

$$PCr + ADP \rightleftharpoons ATP + Cr$$

$$\text{(Anaerobic) Glycogen} + P_i + ADP \longrightarrow ATP + \text{LACTIC ACID}$$

$$\text{(Aerobic) Glycogen/Glucose} + ADP + P_i + O_2 \longrightarrow ATP + H_2O + CO_2$$

(where ATP represents adenosine triphosphate, ADP adenosine diphosphate, $P_i$ inorganic phosphate, Cr creatine, and PCr phosphorylcreatine). The hydrolysis of the high energy phosphate ATP (concentration, 5 m mole $Kg^{-1}$ in muscle) is the immediate source of energy whereas another high energy compound PCr (concentration, 29 m mole $Kg^{-1}$) serves as a high energy buffer to maintain ATP levels during exercise. The consumption of glucose and glycogen provides the ultimate long term sources of energy under conditions of full oxygen (aerobic) and restricted oxygen (anaerobic or ischemic) supply.

The first demonstration of the clinical utility of $^{31}P$ NMR spectroscopy was in the diagnosis of the rare muscle disease, McArdle's syndrome. Phosphorus-31 spectra of the forearms of controls and the McArdle's patients revealed that while ATP levels were maintained in both sets of subjects during aerobic and ischemic exercise, the McArdle's patient suffered a precipitous loss of PCr and a gain of $P_i$ during ischemic exercise. More importantly, the intracellular pH of

the controls measured by $^{31}P$ NMR dropped during ischemic exercise due to anaerobic generation of lactic acid. The muscular pH of the McArdle's patient did not drop, indicating that lactic acid was not being generated due to a deficiency of the enzyme phosphorylase which catalyzes the breakdown of glycogen. This diagnosis of a specific enzyme defect in the exercise intolerance of this patient was confirmed by open muscle biopsy.

Phosphorus-31 NMR spectroscopy can now be used to diagnose a number of muscle diseases including muscular dystrophy and several other enzyme deficiency diseases, including phosphofructokinase deficiency which causes exercise intolerance without the phenomenon of a second wind seen in McArdle's syndrome. These studies of humans have been limited to arms and legs because 1.5 Tesla or higher field superconducting magnets that will accept the human torso are not yet available. These whole body NMR spectroscopy systems are expected to be available later this year, although this may be an overly optimistic projection because there are significant technical problems to be overcome in the design and construction of these large magnet systems. When they do become available, $^{31}P$ NMR investigations of the interior organs of the body are likely to extend significantly the utility of the technique.

In the meantime, the narrower bore (20-30 cm) high field (1.5-2 Tesla) systems are being used to assess the viability of kidneys for transplant and to develop an NMR data base on specific organ systems in animal models. Phosphorus-31 NMR studies of kidneys indicate that those kidneys which show high levels of ATP, low levels of $P_i$, and only moderate increases in acidity after removal from the donor, function better after transplantation. When whole body NMR spectrometers become available, $^{31}P$ NMR spectroscopy will be useful in charting the progress of the kidney after transplantation, allowing early signs of rejection with the signal to increase immunosuppressive therapy.

Among the more thorough $^{31}P$ NMR investigations of an organ are those of heart in a perfused state or in live animal models studied

under normal and ischemic conditions with surface coils and surgically implanted coils to allow probing of spatially localized metabolism. As seen in $^{31}P$ spectra, regional ischemia of heart achieved by ligature of the left descending coronary artery is accompanied by a rapid fall in pH, PCr, ATP, and a rise in the concentration of Pi and sugar phosphates. The $^{31}P$ spectra of hearts treated with drugs, e.g., putative potassium agonists, pre- or post-ligature results in maintenance or regeneration of PCr and ATP levels. These results on ischemic heart, as well as those obtained with anethestized animals and hearts whose contractions have been arrested, lend confidence that $^{31}P$ spectroscopy will provide a non-invasive technique for defining the extent and irreversibility of tissue damage from myocardial infarction and for monitoring the response of infarcted tissue to treatment. It must be stressed, however, that these studies are stil very much in the research phase.

In an even earlier phase of research are NMR spectroscopic studies with substrates enriched with carbon-13. Althougn a few promising NMR studies of naturally occurring $^{13}C$ compounds have been completed with animal models and humans, the methodology is still very much in the research phase with perfused organ models. Carbon-13 NMR spectroscopic studies are being vigorously pursued because: (1) Many important metabolites whose accumulation or diminution might be diagnostic of a metabolic disease or physiological disorder do not contain phosphorus and cannot be detected directly by $^{31}P$ NMR spectroscopy; and (2) the stable $^{13}C$ has a low natural abundance, 1.1 atom %, and substrates labeled with the enriched isotopes can be used as <u>in situ</u> and <u>in vivo</u> tracers. Some studies of perfused heart have been initiated, but the most widely studied organ to date has been the perfused liver with a focus on the important processes of gluconeogenesis, glycogenolysis, and glycogen formation. (Fig. 2).

Recently, the quantitation of the rates of glycogen formation and gluconeogenesis from $^{13}C$ labeled gluconeogenic precursors like [3-$^{13}C$]-L-alanine has been accomplished. In addition, the appearance of different concentrations of the $^{13}C$ label at different positions in

the glucose molecule and in the aspartate and glutamate products of the Krebs cycle, has allowed an assessment of the relative contributions of gluconeogenesis in the cytosol of the cell and of the Krebs cycle in the mitrochondrion, to the consumption of [3-$^{13}$C]-L-alanine. Because the activity of the Krebs cycle is dependent on the oxygen delivery to the liver and gluconeogenic activity is dependent on ATP supply, gluconeogenesis, glycogen formation, and the appearance of $^{13}$C label in aspartate and glutamate should be sensitive functions of oxygen supply. This has been confirmed by $^{13}$C NMR spectroscopic studies of mildly anoxic and hypoxic livers. These $^{13}$C NMR metabolic profiles are very important in assessing liver function, because more classical "wet chemistry" methods suggest that a fall in ATP levels in the liver is a much less sensitive indicator of oxygen up-take than are the rates of glycogen formation, gluconeogenesis and lactate uptake. Comparative $^{31}$P and $^{13}$C NMR spectroscopic studies to assess this are now under way.

It may be possible in the future to combine NMR imaging and NMR spectroscopy. It is problematical whether it will ever be possible to obtain $^{31}$P and $^{13}$C NMR images due to the low concentration of these isotopes in the body. However, it should be possible at high fields to distinguish the small chemical shifts of protons and to extract spectroscopic information from high field proton NMR images. Promising early results have been obtained on forearm, the spectra of lipids and water in bone marrow and muscle having successfully been extracted from the proton NMR image.

The problem areas that must be addressed as NMR spectroscopic studies progress from perfused organ and animal model to human studies are many. High field magnets, 1.5 Tesla or greater, having a one meter bore with a large volume of $H_0$ homogeneity (0.5 to 1 ppm over a 40 cm radius), must be designed, constructed, and put into routine operation. This is a challenging task. Only slightly less challenging will be the design and construction of radiofrequency coils which have a high homogeneity of the $H_1$ field only in a well-defined volume that can be preselected. Intensive work is being carried out in both these areas and progress should be rapid. Motion is a different problem area which

arises from the relatively long signal averaging times required in $^{31}P$ and $^{13}C$ spectroscopy. The degradation of the volume resolution and the magnetic field homogeneity caused by motion, can probably largely be circumvented by synchronizing the rf pulse, e.g. to regular breathing or to beating of the heart. Finally because the body is a magnetically heterogeneous medium, the variations in local bulk magnetic susceptibility will cause a small variable modulation of the $H_o$ field across the body. This modulation will cause a small spread in the chemical shifts for a given compound, and result in some broadening of the lines in the spectrum, an effect which should be bothersome, but not serious.

## IV. POTENTIAL BIOLOGICAL HAZARDS

A key issue in the use of NMR in human studies is whether the static fields, field gradients, or rf irradiation used are "safe". Many years of experience with cyclotrons and NMR instruments which expose operators to large stray fields, have produced no firm evidence of any biological hazard due to static magnetic fields. Such anecdotal evidence is not completely satisfactory and is being followed up by epidemiological studies. Controlled pilot studies on bacterial strains, mammalian cells, cell cultures, and animal models have shown no reproducible effects of exposure to magnetic fields, rf irradiation, or magnetic field gradients commonly employed in NMR. The effects monitored include chromosome abnormalities, lethality, and morphorogical and physiological changes. The modulation of electrocardiograms of the heart by high static magnetic fields has been the cause of some concern, but the EKG changes result from an induced EMF associated with high velocity blood (a conductor) flow through the magnetic field. It is not a physiological effect, no arrhythmias or changes in heart rate being induced and the normal EKG appearing after removal of the animal from the magnetic field. It is generally conceded that biological hazards are unimportant at static fields of 2T or less.

On experimental and theoretical grounds, biological effects of static fields, oscillating field gradients, and rf irradiation at high

values, not in actual or anticipated human use will occur. For example, static magnetic fields of 5 Tesla or greater may cause detectable changes in the conduction velocity of nerves and these experiments will probably be carried out in animal models over the next two to three years. Oscillating field gradients of 500 Tesla per second can induce currents in the body of 500 amperes per $cm^2$ and induce heart fibrillation. Oscillating fields of 1000 T/sec could cause electroanesthesia. Both these values of the oscillating field, and the time it is switched on, are far removed from the conditions used in NMR experiments. As anyone who has operated a microwave oven knows, rf irradiation can cause pronounced biological effects; but the rf fields used in NMR cause only small heating effects. For example, normal NMR rf irradiation deposits energies of the same order of magnitude or the average metabolic waste heat of 1.5 watts/Kg. Even with 20 minutes of normal rf irradiation and with no heat conduction from the irradiated volume by blood flow, the tissue temperature would rise only 1-1.5° C. Nonetheless rf heating effects must be kept in mind for those subjects fitted with prosthetic devices (metallic) that may have high dielectric losses that are converted to localized heating. In the future, use of higher fields will lead to use of higher rf frequency and local heating will need to be measured as a potential hazard.

There are known hazards associated with the interaction of metallic objects with magnetic fields. One of the most important of these derives from the acceleration of ferromagnetic materials in a field gradient. These potential projectiles include wrenches, screw drivers, scalpels, etc. which can acquire high velocities especially in the vicinity of 1.5 Tesla systems. This must be circumvented by controlled access to the NMR facility. Other potential physical hazards, which can be controlled by careful patient and visitor screening, are the resetting of pacemakers by the NMR systems, and the movement of metallic surgical clips which could lead to bleeding. Finally, more subtle hazards are associated with the perturbation of magnetic fields by ferromagnetic materials and the effect of those perturbations on the NMR image. Dark spots on proton NMR images of the

brain have been caused by dental prostheses and steel ribs in wigs, and on NMR images of the pelvic area by steel prosthetic devices.

## V. ACKNOWLEDGEMENTS

The author is grateful for the helpful comments and criticisms of Drs. E. Fukushima and J. Brainard of Los Alamos National Laboratory, Professor T. Budinger of the University of California, Berkeley, and Dr. T. Brady of the Massachusetts General Hospital.

Fig. 1. THE BASIC NMR EXPERIMENT.

A. In the absence of an external magnetic field, there is a random orientation of individual nuclear dipole moments.

B. In the presence of a strong external field, $H_0$, the individual nuclear dipoles tend to orient in a low energy state aligned with the field and precess around it at the Larmor frequency which is proportional to the product of the nuclear magnetic moment and the applied field strength, $W_0 \propto \mu H_0$. Because of the orientation of the individual magnetic moments, a net macroscopic magnetization, $M_0$, is induced along the applied field direction (Z) but, because the individual moments are not precessing in phase, no net magnetization is induced in the xy plane.

C. If a second magnetic field $H_1$, rotating at the Larmor frequency, in the plane perpendicular to the external field, $H_0$, is applied as a short pulse, the macroscopic magnetization is tilted from the Z axis by an angle which depends on the $H_1$ field strength and the duration of the pulse.

D. After termination of the $H_1$ pulse, the net magnetization a $M_0$ precesses freely about $H_0$ at the Larmor frequency and this fluctuating magnetization in the xy plane induces a small voltage change in a sensitive pick-up coil which can be the same coil which transmitted the $H_1$ pulse.

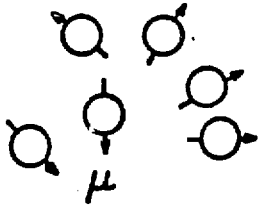
μ

A

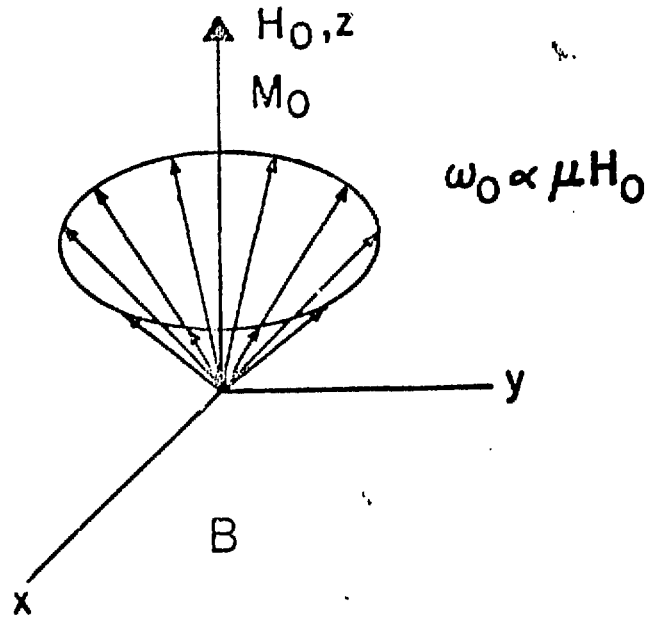
H0,z
M0
ω0 ∝ μH0
y
x

B

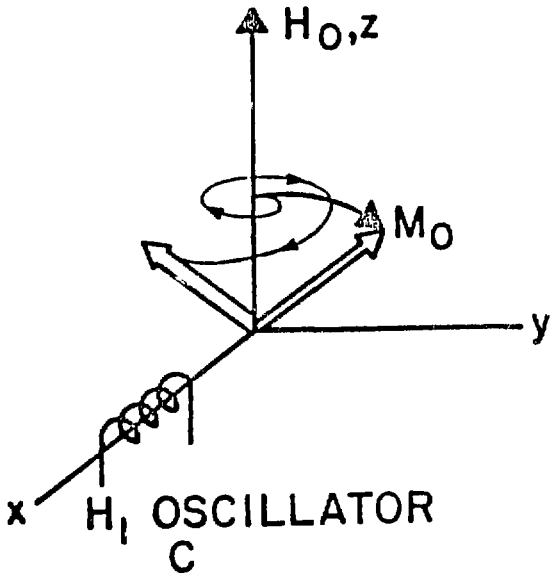
H0,z
M0
y
x
H1 OSCILLATOR

C

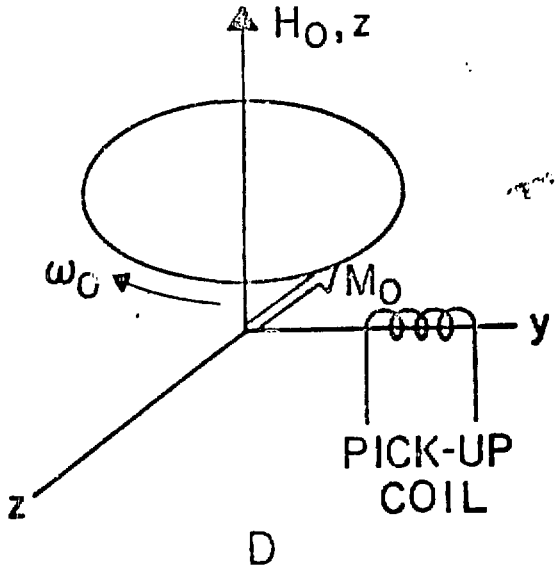
H0,z
ω0
M0
y
z
PICK-UP
COIL

D

Fig. 1

Fig. 2. The $^{13}C$ NMR Spectra of a Syrian Hamster Liver Perfused with a Solution Containing Nutrients and Oxygen. Plotted are the intensities of the resonances as a function of chemical shift. The intensity of the resonance is proportional to its concentration and its chemical shift is a function of chemical environment. Chemical shifts were assigned to specific atoms in specific molecules by comparisons and $^{13}C$ enrichments which are now standard procedures in this field. All of the resonances were assigned but, for the sake of clarity, only a few of the assignments are shown.

A. The background spectrum of the perfused liver shows many overlapping $^{13}C$ resonances for wide varieties of compounds present in the liver cells. Predominant among these are lipids formed by the combination of glycerol, fatty acids $[CH_3(CH_2)_7\overset{H}{C}=\underset{H}{C}(CH_2)_7CO_2H]$, and sometimes choline $[HOCH_2CH_2N(CH_3)^+]$. Assignments of some specific classes of carbon atoms are shown. The electron poor carboxyl groups ($CO_2$) resonate at 180 ppm to the low frequency side of the reference (0 ppm) whereas the more electron rich methyl groups ($CH_3$) at only 15-55 ppm to low frequency side.

B. and C. The spectra were obtained 60 min. and 140 min. after $^{13}C$ enriched compound, [3-$^{13}C$]-L-alanine, was added to the perfusion solution. Some of the assignments made include the very intense resonance of the [3-$^{13}C$] carbon of alanine at ~17 ppm, the [2-$^{13}C$] carbon of glutamate at ~35 ppm and glucose resonances for carbons 1-6 at chemical shifts in the range 55-92 ppm.

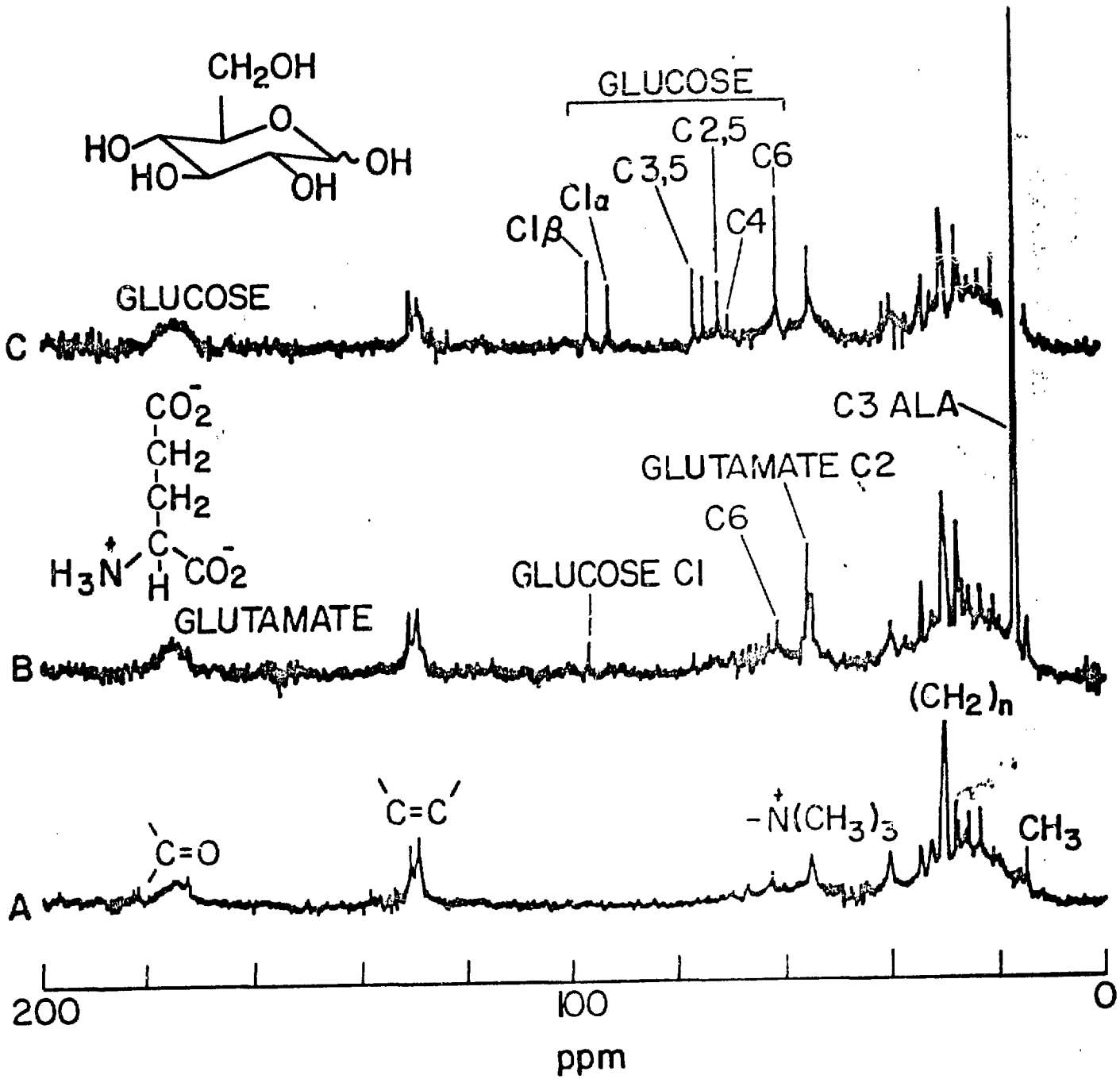
CH2OH
O
HO
HO
OH
OH
GLUCOSE
C 2,5
C 3,5
C6
C1α
C1β
C4
GLUCOSE
C
C3 ALA
CO2
CH2
CH2
C
H3N
H
CO2
GLUTAMATE C2
C6
GLUCOSE C1
GLUTAMATE
B
(CH2)n
C=C
-N(CH3)3
CH3
C=O
A
200
100
0
ppm

Fig. 2

## THE EFFECT OF A ONE DIMENSIONAL MAGNETIC FIELD GRADIENT ON THE SPATIAL VARIATION OF AN $^1H$ NMR SPECTRUM

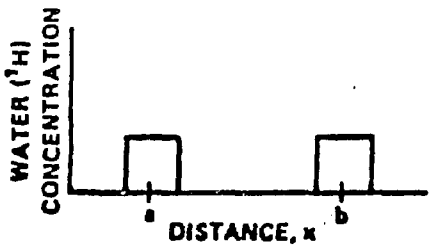


DEPICTED TO THE LEFT ARE TWO BEAKERS OF WATER. WITH NO FIELD GRADIENT, THAT IS $H_0$ IS THE SAME FOR ALL VALUES OF x, THE $^1H$ NMR CONSISTS OF A SINGLE RESONANCE SHOWN AT RIGHT.

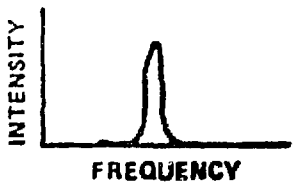


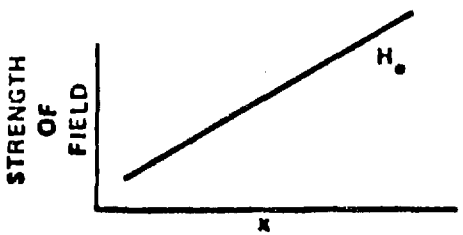


IF THE FIELD GRADIENT SHOWN AT THE LEFT IS APPLIED, THEN FOR SMALL VALUES OF x, THE $^1H$ WILL COME INTO RESONANCE AT LOWER FREQUENCIES THAN AT LARGE VALUES OF x. THE FREQUENCY OF RESONANCE IS THEN A MEASURE OF THE POSITION x. THE RESULTING SPECTRUM IS SHOWN AT RIGHT.

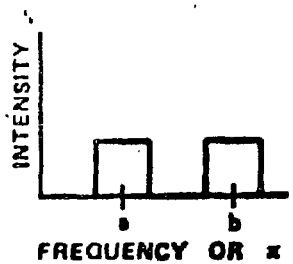


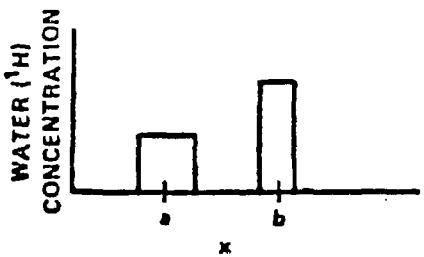


IF THE SAME FIELD GRADIENT IS APPLIED TO DIFFERENT SHAPED BEAKERS SHOWN TO THE LEFT WHICH CONTAIN THE SAME AMOUNTS OF WATER, THEN THE SPECTRUM AT THE RIGHT WILL RESULT.

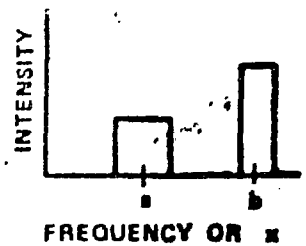


Fig. 3

**Fig. 4. The time dependence of the magnetization of the sample, called relaxation, is due to the interaction of the nuclear magnetic moments with each other and with the fluid, medium, or lattice in which they are moving. These interactions cause a dephasing of the magnetization in the xy plane and a recovery of the magnetization along the Z axis.** These effects are illustrated for magnetization immediately after an $H_1$ pulse has tilted the $M_0$ magnetization vector away from the Z axis (see Fig. 1).

A. Detected signal $M_{xy}$, decays with a characteristic time $T_2$ called the spin-spin relaxation time, because of the dephasing of the individual movements.

B. The macroscopic magnetization, $M_0$ or $M_Z$, recovers with a characteristic time constant $T_1$, called the spin lattice relaxation time, due to the transfer of energy between the spins and the lattice. $T_1$ and $T_2$ may be the same or different. In this case $T_2 < T_1$.

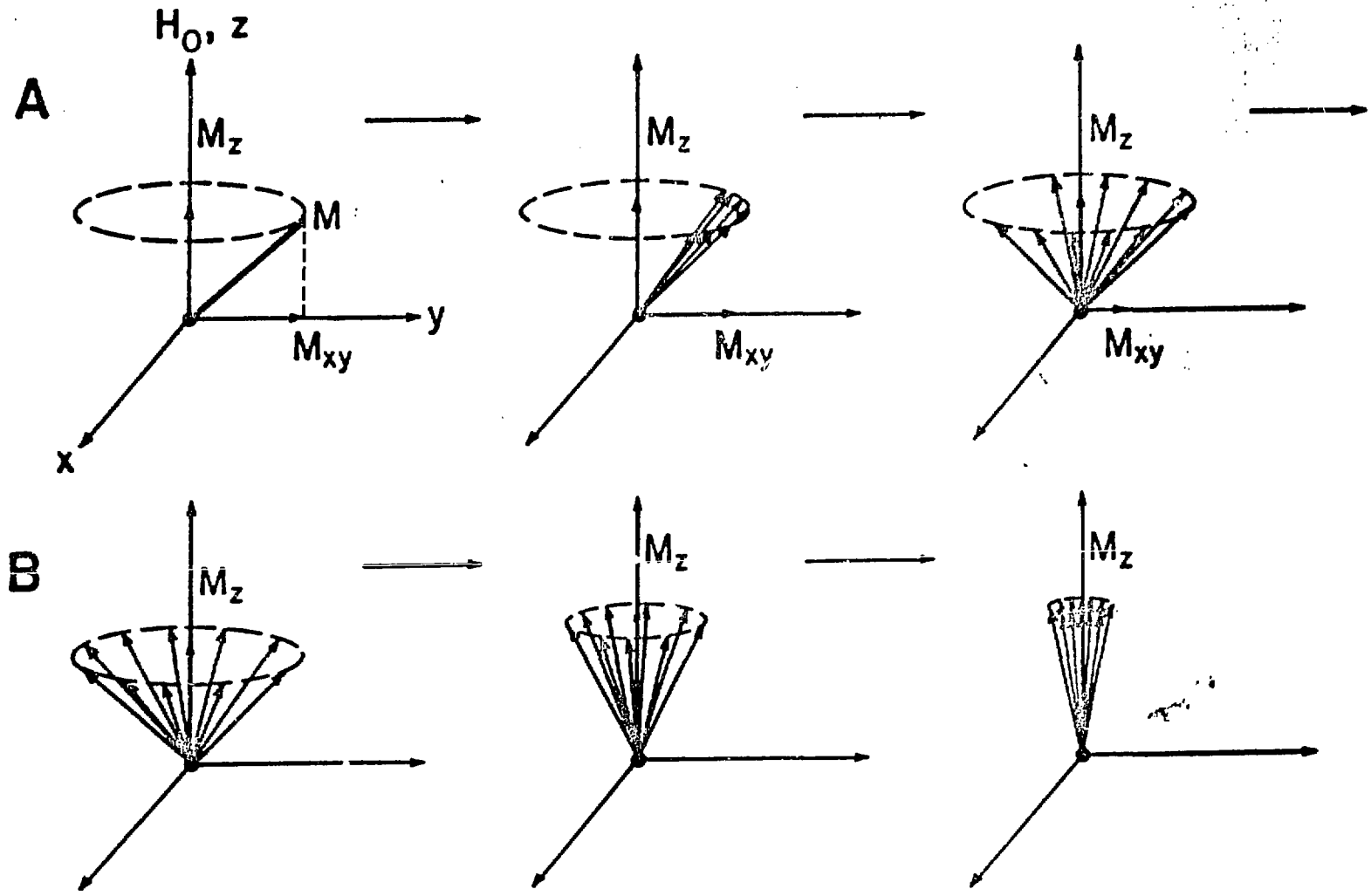


Fig. 4

Fig. 5. Image Enhancement by $T_1$ Weighting.

A. Recovery of the magnetization, $M_0$, of the mobile protons in brain and cerebral spinal fluid (CSF). The mobile protons in brain have a shorter $T_1$, than those of CSF, that is the $M_0$ of brain recovers along the Z axis (Fig. 4) much faster after an $H_1$ pulse tilts $M_0$ into the xy plane. If the next pulse in the signal averaging experiment is applied in a time long compared with $T_1$ (point 1 on the plot), $M_0$ for both brain and CSF have recovered to their equilibrium values and full signal intensity for both is recovered from the next pulse. If, however, the next pulse is delivered in a time long compared with brain $T_1$ but short with respect to CSF $T_1$ (point 2 on the plot), then the effect is to attenuate the mobile proton signals from CSF and enhance proton image contrast as shown in the schematic images (1) and (2).

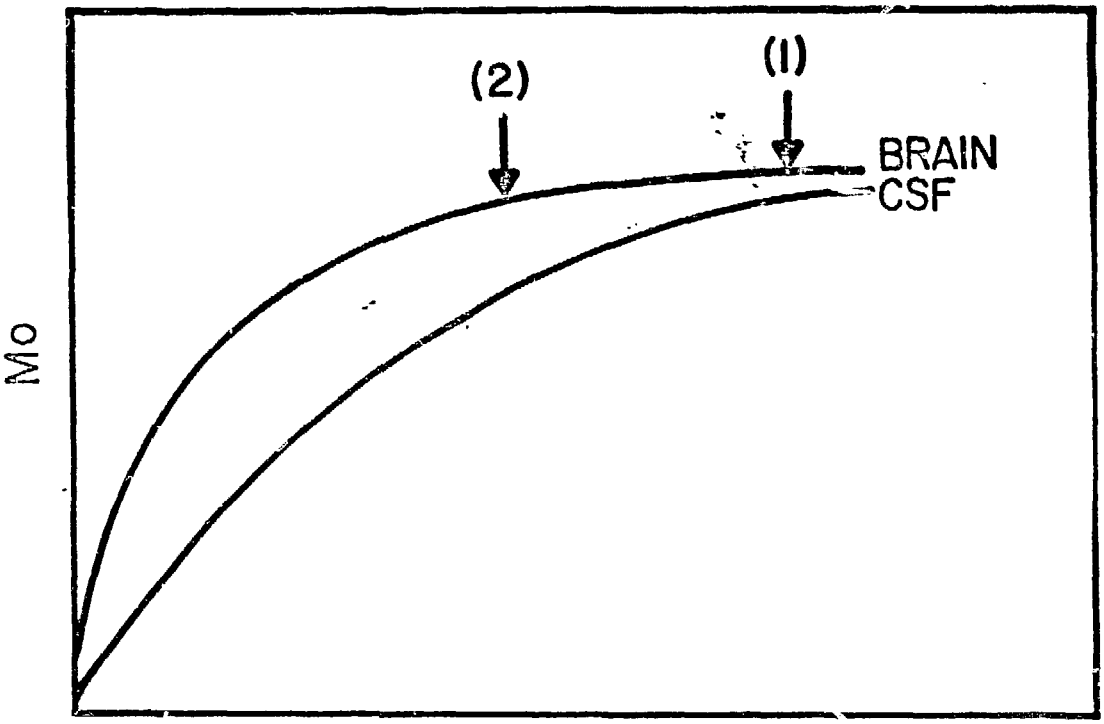


A

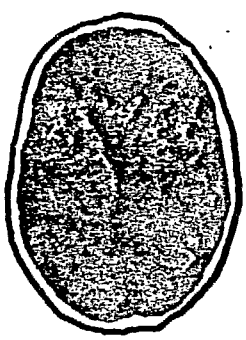

(1)

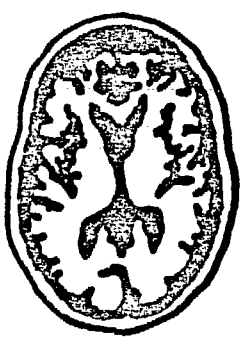

(2)

Fig. 5

## SELECTED BIBLIOGRAPHY


1. R. E. Gordon, P. E. Hanley, and D. Shaw, "Topical Magnetic Resonance in Progr. in Nucl. Mag. Res. Spec., 15, 1-47 (1982).

2. I. L. Pykett, J. H. Newhouse, F. S. Buonanno, T. J. Brady, M. R. Goldman, J. P. Kistler, and G. M. Pohost, "Principles of NMR Imaging," Radiology, 143, 157-168 (1982).

3. L. E. Crooks, C. M. Mills, P. L. Davis, J. Hoenninger, M. Arakawa, J. Watts, and L. Kaufman, "Visualization of Cerebral and Vascular Abnormalities by NMR Imaging. The Effects of Imaging Parameters on Contrast," Radiology, 144, 842-852 (1982).

4. I. R. Young, A. S. Hall, C. A. Pallis, N. J. Legg, G. M. Bydder, and R. E. Steiner, "NMR Imaging of the Brain in Multiple Sclerosis," Lancet, 2 (8255), 1063-1066 (1981).

5. D. G. Taylor and C. F. Bare, "A Review of the Magnetic Resonance Response of Biological Tissue and Its Applicability to the Diagnosis of Cancer by NMR Radiology," Comp. Tomog., 5, 122-173 (1981).

6. T. F. Budinger, "Nuclear Magnetic Resonance (NMR) In Vivo Studies: Known Thresholds for Health Effects," J. Comp. Assn. Tomog., 5, 800-811 (1981).

7. R. H. T. Edwards, M. J. Dawson, D. R. Wilkie, R. E. Gordon, and D. Shaw, "Clinical Use of NMR in the Investigation of Myopathy," Lancet, March 27, 1982, pp. 725-731.

8. F. W. Smith, A. H. Adams, and W. D. P. Phillips, "NMR Imaging in Pregnancy," Lancet, Jan. 1, 1983, 61-62.

9. J. J. H. Ackerman, T. H. Grove, G. G. Wong, D. G. Gadian, and G. K. Radda, "Mapping of Metabolites in Whole Animals by $^{31}P$ NMR Using Surface Coils," Nature, 167-170 (1980).

10. R. D. Ross, G. K. Radda, D. G. Gadian, G. Rocker, M. Esiri, J. Falconer-Smith, "Examination of a Case of Suspected McArdle's Syndrome by $^{31}P$ NMR," N. Engl. J. Med., 304, 1338-1342 (1981).

11. D. G. Gadian, G. K. Radda, R. D. Ross, J. Hockaday, P. J. Bore, D. Taylor, P. Styles, "Examination of a Myopathy by $^{31}P$ NMR," Lancet, 774-775 (1981).

12. B. Chance, S. Eleff, J. S. Leigh, D. Sokolow, A. Sapega, "Mitochondrial Regulation of Phosphocreatine/Phosphate Ratios in Exercising Human Limbs, Gated $^{31}P$ NMR Study," Proc. Natl. Acad. Sci. (USA), 78, 6714-6718 (1981).

13. T. C. Ng, W. T. Evanochko, R. N. Hiramoto, V. K. Ghanta, M. B. Lilly, A. J. Lawson, T. H. Corbett, J. R. Durant, and J. D. Glickson, "$^{31}P$ NMR Spectroscopy of in vivo Tumors," J. Magn. Res., 49, 271-286 (1982).

14. N. A. Matwiyoff, R. E. London, and J. Y. Hutson, "The Study of the Metabolism of $^{13}C$ Labeled Substrates by $^{13}C$ NMR spectroscopy of Intact Cells, Tissues, and Organs," American Chemical Society Symposium Series, 191, 157-186 (1982).

15. J. R. Brainard, J. Hutson, R. E. London, and N. A. Matwiyoff, "Enriched Stable Isotopes and NMR Spectroscopy in Metabolism," Los Alamos Science, Summer 1983.

16. R. G. Shulman, "NMR Spectroscopy of Living Cells," Scientific American, 248, 86-93 (1983).

17. J. R. Alger, L. O. Sillerud, K. L. Behar, R. J. Gillies, R. G. Shulman, R. E. Gordon, D. Shaw, and P. E. Hanley, "In Vivo $^{13}C$ NMR Studies of Mammals," Science, 214, 660-662 (1981).

18. R. L. Nunnally and P. A. Bottomley, "Assessment of Pharmacological Treatment of Myocardial Infarction by Phosphorus-31 NMR with Surface Coils," Science, 211, 177-180 (1981).